

# Quaternized chitosan/montmorillonite nanocomposite resin and its adsorption behavior

Jiwen Luo<sup>1,2</sup> · Guocheng Han<sup>1</sup> · Meijia Xie<sup>2</sup> · Zhou rong Cai<sup>3</sup> · Xiaoying Wang<sup>1</sup>

Received: 2 December 2014 / Accepted: 3 May 2015 / Published online: 12 May 2015  
© Iran Polymer and Petrochemical Institute 2015

**Abstract** Chitosan was intercalated into a layer of montmorillonite to obtain a chitosan/montmorillonite nanocomposite. The chitosan/montmorillonite nanocomposite resin was prepared via inverse suspension method. Finally, a novel quaternized chitosan/montmorillonite nanocomposite resin was fabricated using the nanocomposite resin as raw material and 2,3-epoxypropyltrimethyl ammonium chloride as quaternized ammonium modifier. The structure and the morphology of chitosan/montmorillonite nanocomposite and quaternized chitosan/montmorillonite nanocomposite resin were characterized by X-ray diffractometry, transmission electron microscopy, Fourier transform-infrared spectroscopy, scanning electron microscopy and confocal laser-scanning microscopy. The results show that the quaternized chitosan/montmorillonite nanocomposite resin possessed smooth surface, regularly spherical shape, dense structure and good dispersibility in water, with average diameter of 14–113  $\mu\text{m}$ . The low swelling behavior of quaternized chitosan/montmorillonite nanocomposite resin was helpful to its use in column packing. The adsorption results on methyl orange revealed that the quaternized chitosan/montmorillonite nanocomposite resin exhibited stronger adsorption capacity in comparison with quaternized chitosan

resin without montmorillonite, and the adsorption capacity increased along with the increasing amount of montmorillonite. The maximum adsorption capacity of quaternized chitosan/montmorillonite nanocomposite resin was 478.5  $\text{mg g}^{-1}$  and the adsorption behavior could be well described by the Langmuir and Freundlich adsorption isotherm model. Therefore, this study may provide a considerable and prospective material in the field of wastewater treatment.

**Keywords** Chitosan · Montmorillonite · Quaternized chitosan · Resin · Adsorption

## Introduction

Chitosan, a deacetylated derivative of chitin, is the second largest renewable resource in nature. Chitosan shows strong adsorption capacity for the existence of amino and hydroxyl groups, which enable it to remove impurities effectively. Moreover, because of its biodegradability, chitosan and chitosan-based nanocomposites are popular and widely used in film fabrication [1], biomedical applications [2, 3], water treatment [4] and many other fields [5–7]. However, when used in column packing, chitosan in the form of flake or powder is prone to bring about column pressure, which results in lowering of the operational efficiency [8] and dissolution in acid solution. Therefore, chitosan resin is attracting more attention because of its good usage as absorbent. In order to improve its selectivity and capacities, Qin et al. introduced quaternary ammonium groups on the chitosan resin, which showed good adsorption capacity in a wider pH range [9]. However, compared to other strong absorbents, the removal capacity of quaternized chitosan resin is not satisfactory.

✉ Xiaoying Wang  
xyw@scut.edu.cn

<sup>1</sup> State Key Laboratory of Pulp and Paper Engineering, South China University of Technology, Guangzhou 510640, People's Republic of China

<sup>2</sup> Key Laboratory of Theoretical Chemistry of Environment Ministry of Education, School of Chemistry and Environment, South China Normal University, Guangzhou 510006, People's Republic of China

<sup>3</sup> School of Marine Sciences, Sun Yat-Sen University, Guangzhou 510006, People's Republic of China

For this point, layered silicates such as montmorillonite (MMT) and rectorite have achieved special attention, as they are the most commonly used adsorbents in the removal of organic pigments and dyes due to their high surface area and high cation exchange capacity [10, 11]. Many studies have revealed that MMT can improve the physicochemical characteristics of chitosan or chitosan derivatives [12, 13]. In our previous study [14], it was indicated that the preparation of quaternized chitosan/organo montmorillonite (QCS/OMMT) nanocomposites was rapid by intercalating quaternized chitosan into the interlayer of OMMT. The results showed that an optimum flocculability concentration of QCS/OMMT nanocomposites was only  $0.005 \text{ mg L}^{-1}$ , which was much lower than that of quaternized chitosan ( $15 \text{ mg L}^{-1}$ ). Moreover, the QCS/OMMT nanocomposites showed a stronger antimicrobial activity than quaternized chitosan because of fine dispersion and interaction between quaternized chitosan and OMMT [15]. Moreover, compared to pure quaternized chitosan nanoparticles, montmorillonite loaded on quaternized chitosan enhanced the drug encapsulation efficiency of the nanoparticles and slowed the drug release from the nanocomposites [16]. However, until now, there is hardly a report about the improved adsorption behavior of quaternized chitosan after the addition of MMT, a resin-based quaternized chitosan/MMT nanocomposite, which is still not exclusively studied.

In this paper, firstly, chitosan was intercalated into the interlayer of MMT under microwave irradiation and the obtained chitosan/MMT nanocomposite was prepared as a resin via inverse suspension method. Then, a novel quaternized chitosan/MMT nanocomposite resin (QCMR) was prepared under the reaction between chitosan/MMT nanocomposite resin and 2,3-epoxypropyltrimethyl ammonium chloride. The structure and the morphology of the nanocomposite and the resin were characterized. Moreover, the adsorption behavior of QCMR for methyl orange was discussed.

## Experimental

### Materials and equipment

Chitosan was purchased from Jinan Haidebei Marine Bio-engineering Co., Ltd. (Shandong, China). The weight average molecular weight ( $M_w$ ) of chitosan was  $3.0 \times 10^5$  and the degree of deacetylation was 80 %. 2,3-Epoxypropyltrimethyl ammonium chloride was purchased from Dongying Guofeng Fine Chemical Co., Ltd. (Shandong, China). Sodium-based montmorillonite (MMT) was purchased from Chengdu XiYa Chemical Technology Co., Ltd. (Chengdu), with cation exchange capacity of 87 mmol/100 g. All other chemicals were of analytical grade.

An XH-100A microwave synthesis system was purchased from Beijing XiangHu Sci.-Tech. Dept. Co., Ltd. (Beijing, China). The microwave power ranged from 100 to 1000 W and the highest reaction temperature was  $300 \text{ }^\circ\text{C}$ .

### Preparation

#### *Preparation of chitosan/MMT nanocomposite*

Chitosan/MMT nanocomposites were prepared via the intercalation of chitosan into MMT. 1 % (w/v) MMT suspension and 1 % (w/v) chitosan solution were prepared in water, respectively. The chitosan solution was dropped slowly into the MMT suspension and reacted under microwave irradiation (800 W,  $80 \text{ }^\circ\text{C}$ ) for 70 min. Finally, chitosan/MMT nanocomposite was obtained after freeze-drying at  $-40 \text{ }^\circ\text{C}$ . The obtained chitosan/MMT nanocomposites with different weight ratios of chitosan to MMT (12:1, 20:1 and 50:1) were labeled as CM1, CM2 and CM3, respectively.

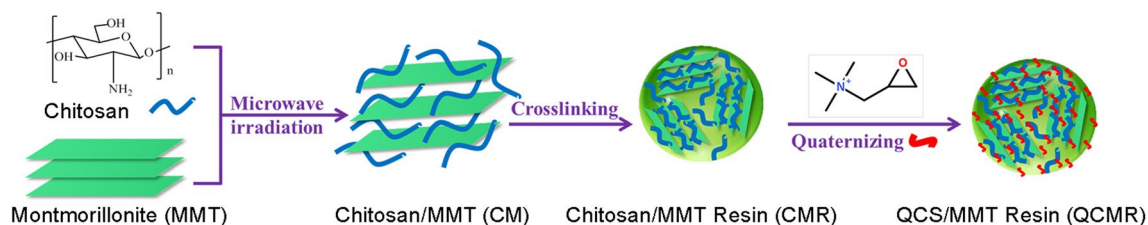
#### *Preparation of chitosan and chitosan/MMT nanocomposite resins*

Chitosan resins were prepared as follows: 3 g chitosan was dissolved into 2 % acetic acid to obtain a 5 % solution, and then 0.1 g PEG2000, 50 mL paraffin oil and 0.3 mL Tween 80 were added as oil phase dispersion media. After the mixture was stirred at room temperature for 1 h, 40 % (v/v) formaldehyde solution was added. The mixture was continuously stirred for 2 h before pouring into 10 % NaOH/ethanol (1:1, v/v) solution, and then the mixture was filtered and washed with petroleum ether and ethanol sequentially. The obtained resins were suspended in 0.067 M NaOH solution. After adding epichlorohydrin as crosslinking reagent, the resin suspension was heated at  $45 \text{ }^\circ\text{C}$  for 3 h, followed by filtering and washing. The new products were dispersed in 0.5 M HCl in order to remove protecting groups. After 12 h, the products were filtered, washed, and then soaked in 5 % NaOH solution for 5 h. Finally, after filtering and washing with water and ethanol sequentially, the chitosan resins were obtained and marked as CSR.

The preparing method of three chitosan/MMT nanocomposite resins was similar to that of chitosan resins, using chitosan/MMT nanocomposite as raw material, and the products were designated as CMR1, CMR2 and CMR3, respectively.

#### *Preparation of quaternized chitosan resins and quaternized chitosan/MMT nanocomposite resins*

Quaternized chitosan resins were also prepared based on chitosan resin via quaternizing reaction. The above



**Scheme 1** Preparation process of QCS/MMT nanocomposite resin

chitosan resin was dispersed in deionized water, and stirred at 60 °C for 24 h after adding 1 mol of 2,3-epoxypropyl-trimethyl ammonium chloride. Quaternized chitosan resins were obtained after washing by deionized water and marked as QCSR.

The preparing method of three quaternized chitosan/MMT nanocomposite resins was similar to that of quaternized chitosan resins, using three kinds of chitosan/MMT nanocomposite as raw materials, followed by crosslinking and quaternizing processes. The products were designated as QCMR1, QCMR2 and QCMR3, respectively. A schematic preparation process of QCMR is shown in Scheme 1.

## Characterization

The *d*-spacing and the structure of chitosan/MMT nanocomposite were investigated by using a D8 advanced X-ray diffractometer (Bruker, Germany) with a  $\text{CuK}\alpha$  radiation ( $\lambda = 0.15418$  nm) at 40 kV and 50 mA. The relative intensity was recorded in the scattering range of  $1^\circ$ – $10^\circ$  and  $5^\circ$ – $90^\circ$  ( $2\theta$ ) at a scanning rate of  $1^\circ$  and  $4^\circ \text{ min}^{-1}$ , respectively. The *d*-spacing was calculated by using Bragg's equation as Eq. (1).

$$n\lambda = 2d \sin \theta \quad (1)$$

where *n* is an integer ( $n = 1$ );  $\lambda$  is the wavelength of incident wave ( $\lambda = 0.15418$ ); *d* is the spacing between the planes in the atomic lattice and  $\theta$  is the angle between the incident ray and the scattering planes.

A JEM-2010HR transmission electron microscope (TEM) (JEOL, Japan) was used to investigate the microstructural morphology of chitosan/MMT nanocomposites at an accelerating voltage of 200 kV. TEM samples were prepared by cutting from the epoxy block with the embedded nanocomposites sheet at room temperature using a Leica UCL/FC6 (Leica, Australia). A few drops of suspended layered silicates were placed on copper mesh grids, and then dried in an oven at 50 °C for 10 min.

FTIR spectra were measured by a Nicolet FT-IR 5700 spectrophotometer (Madison, America) by a KBr pellets method. The spectra were collected for each measurement

over the spectral range 4000–400  $\text{cm}^{-1}$  with a resolution of 4  $\text{cm}^{-1}$ .

The surface morphology of the resins was obtained by a S-3700 N scanning electron microscope (SEM) (Hitachi, Japan). The samples were mounted on metal grids using double-sided adhesive tape, and coated with gold under vacuum.

The morphology of the resins was also observed by a confocal laser-scanning microscope (CLSM, Leica TCS-SP5, Germany). The resins were dyed with fluorescein isothiocyanate (FITC), dispersed in deionized water and treated by ultrasound for 1 min. Afterwards, the resin suspension was dropped onto the glass slide, observed and photographed using argon exciter at wavelength of 488 nm.

## The swelling behavior of the resins

Quaternized chitosan resin and QCMR samples with the same quality were soaked in solutions of different pH values (2, 5, 7, 10 and 12) for 3 h, the surface water of the resins was absorbed by filter paper after filtration, and the wet resins were weighed. The swelling degree (*Sw*) was calculated according to Eq. (2).

$$Sw = \frac{(W_t - W_0)}{W_0} \quad (2)$$

where  $W_t$  and  $W_0$  represent the weight of wet resin and dry resin, respectively.

## The adsorption behavior of the resins

The influences of adsorbent dosage and initial concentration of the dye solution on adsorption of anionic dye methyl orange were investigated, respectively. At 25 °C, 30 mL of methyl orange solution was placed in a 100 mL conical beaker in dark. After adding the resins, the conical beaker was continuously oscillated in the thermostatic water bath oscillator. At proper time intervals, 1 mL of each sample was withdrawn from the solution and immediately back after measuring the absorbency at 464 nm by a UV–Vis spectrophotometer. Each experiment was repeated

three times and the mean values were reported. Both volatilization and photochemical decomposition of the methyl orange were negligible during adsorption experiments [17]. The adsorption amount ( $q_t$ ) was calculated according to Eq. (3).

$$q_t = \frac{(C_0 - C_t)V}{W} \quad (3)$$

where  $C_0$  is the initial concentration of methyl orange ( $\text{mg L}^{-1}$ );  $C_t$  is the concentration of the supernatant in certain time;  $W$  is the weight of the resin;  $V$  is the volume of methyl orange.

## Results and discussion

### Structure and morphology of chitosan/MMT nanocomposite

Figure 1a shows the XRD patterns of chitosan, MMT and chitosan/MMT nanocomposites from  $1^\circ$  to  $10^\circ$ , and the given interlayer distances were calculated by the Bragg's equation. From the figure, original MMT showed  $d_{001}$  basal spacing of 1.42 nm. After intercalation with chitosan, the interlayer distance of MMT was enlarged to 1.48–1.55 nm. Moreover, the  $d_{001}$  spacing of the nanocomposites was negatively proportional to the amount of MMT. The result indicates that chitosan chain was intercalated into the interlayer of MMT [18].

From the XRD patterns from  $5^\circ$  to  $45^\circ$  in Fig. 1b, it is clear that the crystallinity of chitosan was gradually destroyed as the content of MMT increased. Nevertheless, the diffraction peaks of the crystal did not shift, indicating that the structure of chitosan was not changed. The previous study found that the high crystallinity of materials was mainly due to a large number of intermolecular hydrogen bonds [19]. So in view to the degradation of the crystallinity, it can be deduced that the hydrogen-bonds interaction within chitosan was destroyed tremendously after its intercalation into MMT layer, but the structure of chitosan was not changed.

The TEM images in Fig. 2 detail the microstructure of chitosan/MMT nanocomposite, which are the direct information of the intercalation. The dark lines correspond to clay layers, while the bright area represents the intercalated chitosan matrix. As shown in Fig. 2, the characteristic layered structure of MMT can be seen clearly, which remained well-ordered after the intercalation of chitosan. From the lower magnification image in Fig. 2a, there was no obvious aggregation of clays, demonstrating that the layered clays were dispersed well in the chitosan matrix. From the magnified area in Fig. 2b, the obvious enlarged  $d_{001}$  spacing can be observed, where the detailed interlayer distance could be measured. The mean value of layer spacing analyzed by TEM was about 1.5 nm, which is in agreement with

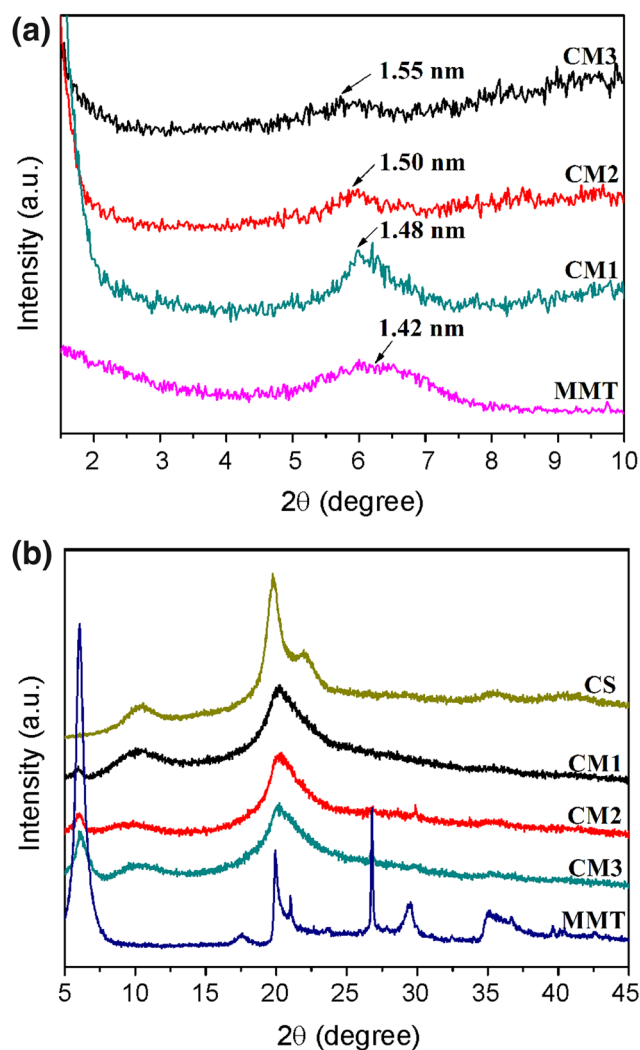


**Fig. 1** XRD patterns of MMT and chitosan/MMT nanocomposites: **a** The small-angle and **b** The wide-angle

the result from the XRD and further confirms the enlarged basal spacing of MMT after intercalation of chitosan.

### Structure and morphology of the resins

The structure of dry resin was analyzed by FTIR spectra as shown in Fig. 3. In the spectra of quaternized chitosan resins, the band at  $1590\text{ cm}^{-1}$  belonging to  $\text{NH}_2$  groups in chitosan resins has disappeared, a new methyl absorption band belonged to quaternary ammonium groups has emerged at  $1483\text{ cm}^{-1}$  [20]. The result indicates that the quaternized modification on chitosan resins has happened. Moreover, compared with quaternized chitosan resin, the spectrum of QCMR1 shows adsorption band of montmorillonite, they were Si-O-Si and Al-O-Si bending vibration bands at  $527$  and  $472\text{ cm}^{-1}$ , respectively [21]. It indicates that MMT was included in the resins.



**Fig. 2** TEM images of chitosan/MMT nanocomposite (CM1)

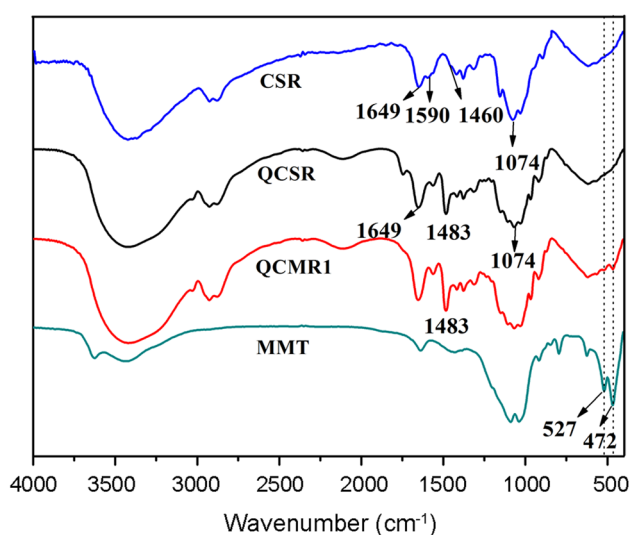
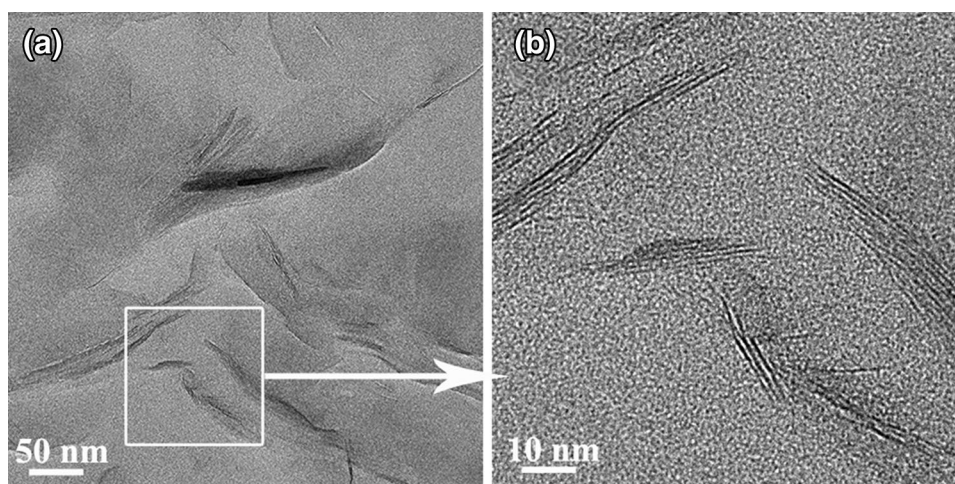


**Fig. 3** FTIR spectra of CSR, QCSR, QCMR1 and MMT

The morphology of dry resins is shown in Fig. 4. It can be observed from Fig. 4a that the resins were regularly spherical with sizes between 14–113  $\mu\text{m}$ . From Fig. 4b, the resins had smooth surface and dense structure. A more microscopic structure can be seen from Fig. 4c that there were more voids in the interior of the resins. Therefore, the prepared QCMR1 had porous structure and a large specific surface area, and these characteristics would benefit the adsorption of dyes or something else [22]. Figure 4d shows the CLSM micrograph of QCMR1 in water, which proves that the resins had better shape and dispersibility in water.

#### Swelling behavior of the nanocomposite resin

The acidity or alkalinity of solution has an effect on swelling behavior of the resin. As shown in Fig. 5, swelling degree of several kinds of resin is decreased with the

increase of pH values because of the presence of quaternized groups [23]. Similar to other positively charged ammonium groups, the quaternized groups exist in the form of salts in acidity, which results in the repulsion between charges and so the molecules are stretched [24]. In addition, it is noteworthy that the swelling degree of QCMR1 was lower than that of quaternized chitosan resin. It shows that the swelling degree of the resin is reduced with the addition of montmorillonite, and this swelling behavior is more conducive to column packing [25].

#### Influence of adsorbent dose on methyl orange adsorption

The effect of dosage of different adsorbents (0.01, 0.02 and 0.04 g) on methyl orange ( $600 \text{ mg L}^{-1}$ ) adsorption amount is illustrated in Fig. 6. The figure shows that unit adsorption amount is increased with the increased amount of adsorbent. When the adsorbent dosage of quaternized chitosan resin was 0.04 g, the equilibrium adsorption capacity was  $167.3 \text{ mg g}^{-1}$ . Compared with quaternized chitosan resin, QCMR1 has a higher equilibrium adsorption capacity. When the mass ratios of quaternized chitosan to MMT were 50:1, 20:1 and 12:1, the equilibrium adsorption capacities of 0.04 g adsorbents were 203.3, 209.3, 215.2  $\text{mg g}^{-1}$ , respectively. It reveals that the adsorption effect of composite adsorbent with MMT is significantly better than that of the pure adsorbent without MMT. And QCMR1 is the optimum one. Since MMT is well known as strong adsorbent [26], the adsorption capacity of the resins becomes stronger when MMT amount is increased.

#### Influence of initial methyl orange concentration on adsorption capacity

At 30  $^{\circ}\text{C}$ , the adsorption isotherm of QCMR1 on the adsorption of methyl orange (200 to 1000  $\text{mg L}^{-1}$ ) was

**Fig. 4** SEM images (a, b, c) and CLSM micrograph (d) of QCMR1

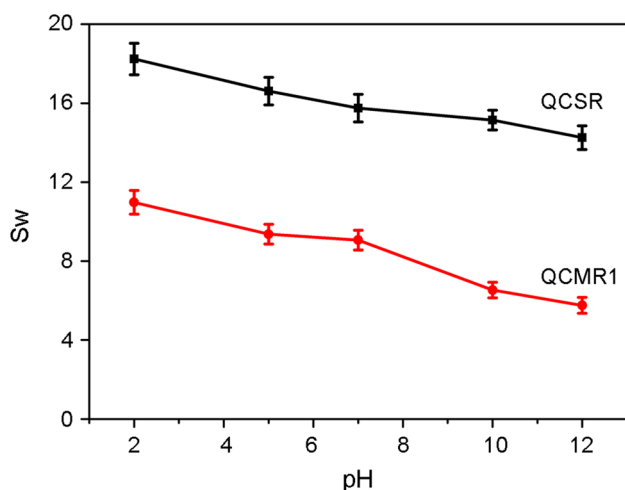
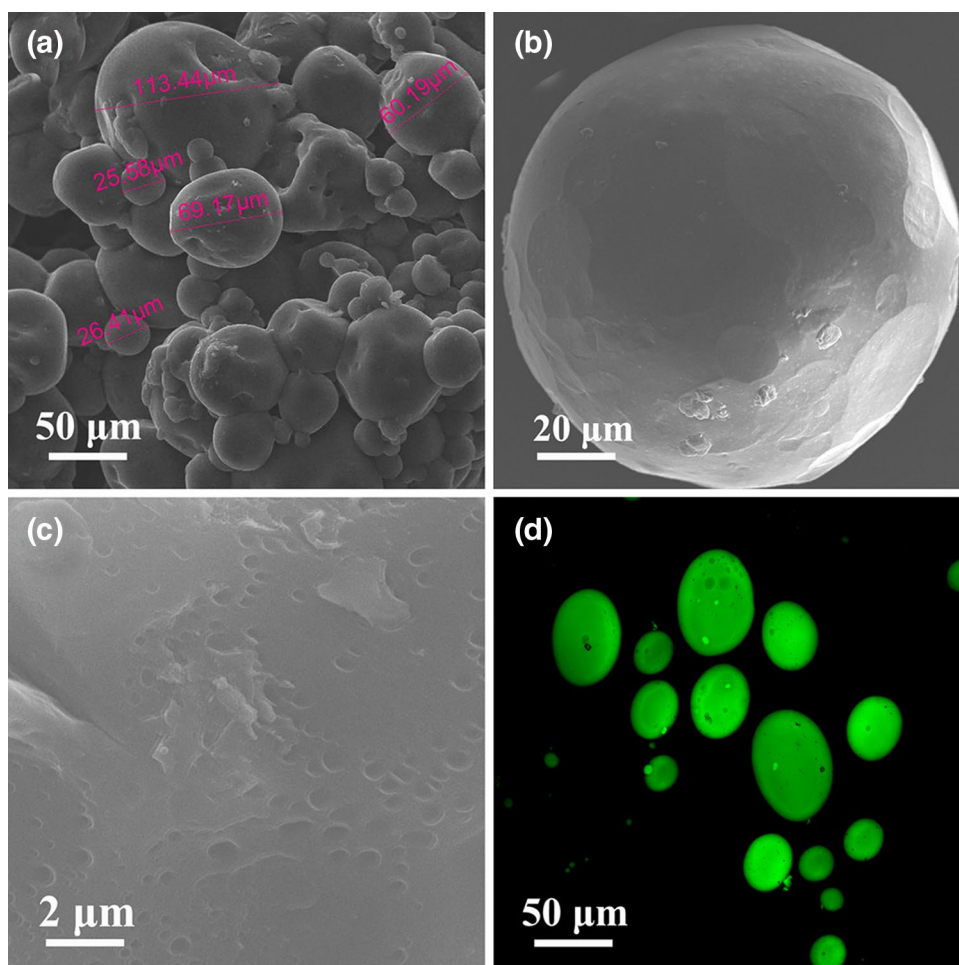


**Fig. 5** Swelling degree of QCSR and QCMR1 with the increase of pH values

examined as shown in Fig. 7a. As can be seen from the diagram, the adsorption capacity is gradually increased with the increasing initial concentration of methyl orange.

Within the range of definite concentration, isothermal adsorption model may be obtained by fitting these experimental data under the experimental temperature.

Langmuir adsorption isotherm assumes monolayer adsorption of adsorbate over a homogeneous adsorbent surface with finite number of identical sites, which are energetically equivalent with negligible interaction between the adsorbed molecules [27]. The Langmuir adsorption isotherm in the linear form is expressed by Eq. (4).

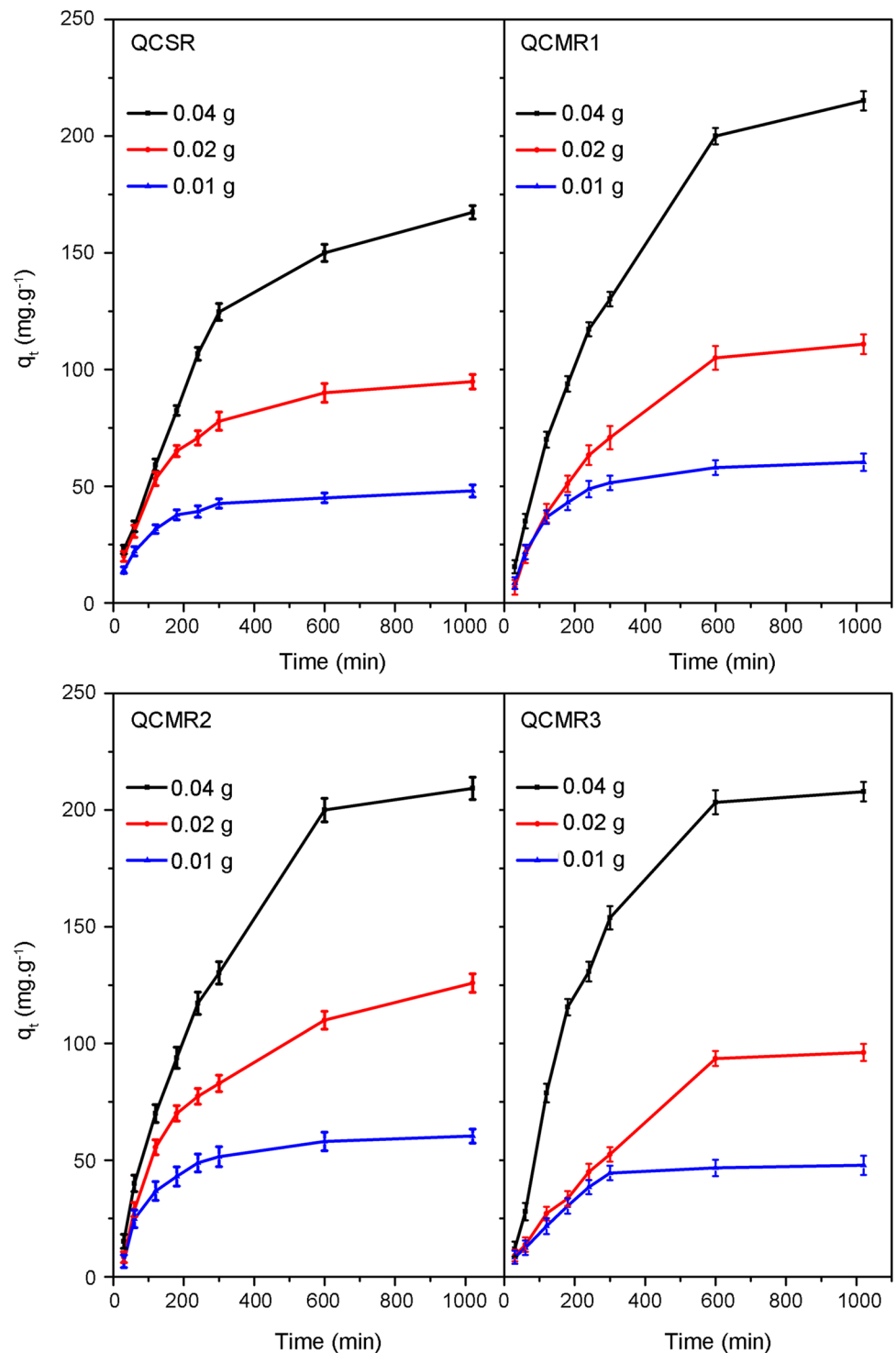
$$\frac{C_e}{Q_e} = \frac{C_e}{Q_m} + \frac{1}{mQ_m} \quad (4)$$

Freundlich adsorption isotherm assumes multilayer adsorption and it is applicable to adsorption on heterogeneous surfaces with interaction between the adsorbed molecules [27]. The Freundlich isotherm is expressed by Eq. (5).

$$\ln Q_e = \frac{1}{n} \ln C_e + \ln k \quad (5)$$

where  $k$  is the Freundlich adsorption constant which roughly indicates the adsorption capacity of the adsorbent

**Fig. 6** Influence of the resin dosage on methyl orange adsorption



and  $n$  is the Freundlich exponent which is related to adsorption intensity.

The experiment data were simulated by Langmuir and Freundlich equation and the results are shown in Fig. 7b and c, respectively. From the graphs, it is evident that the adsorption behavior of nanocomposite resin for methyl orange could be fitted by two kinds of isothermal

adsorption correspondingly, which had a high correlation coefficient ( $R^2 > 0.99$ ) under the range of certain concentration. In addition, Langmuir isotherm was better to describe the adsorption behavior of the resins. The results indicate that the nanocomposite resin on the adsorption behavior of methyl orange might be a monolayer adsorption reaction within the range of certain concentration, and

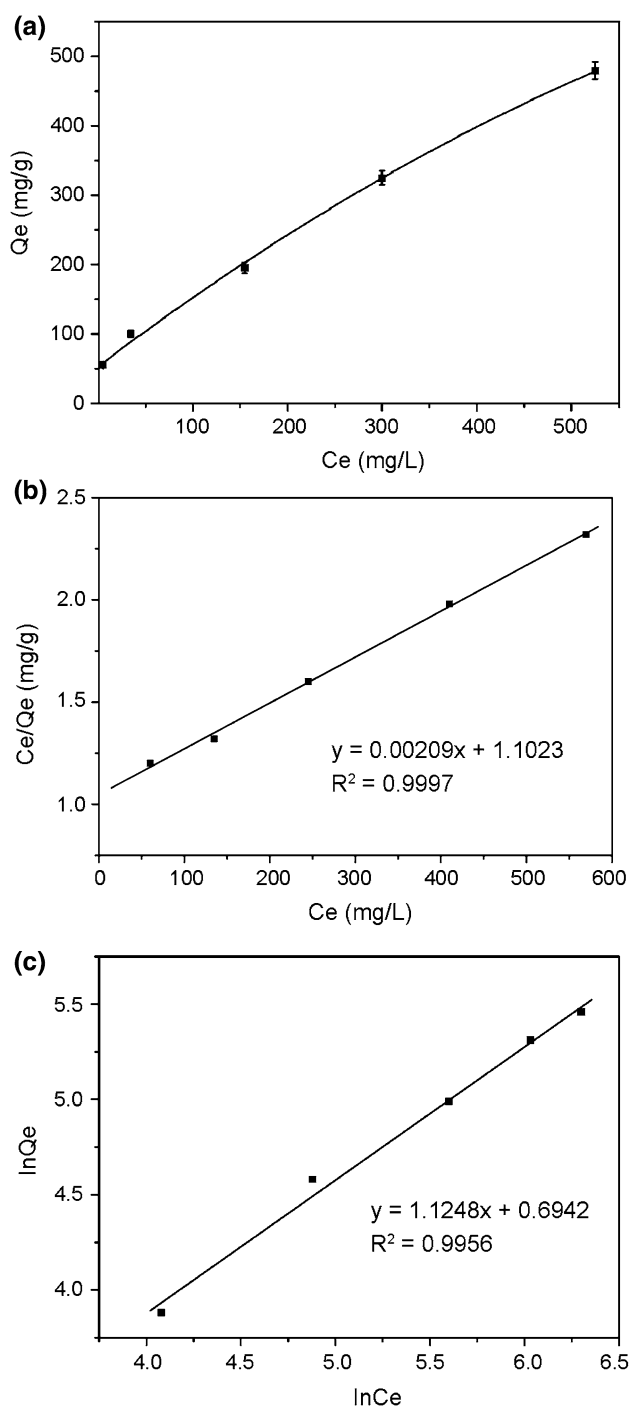


**Fig. 7** **a** Effect of initial methyl orange concentration on adsorption capacity; **b** Langmuir isotherm model; **c** Freundlich isotherm model of adsorption of methyl orange

the isothermal adsorption process can be well described by Langmuir and Freundlich isotherm [28]. The theoretical maximum adsorption capacity of QCMR was  $478.5 \text{ mg g}^{-1}$ . A comparison of adsorption capacities among QCMR1 and other adsorbents is listed in Table 1. When compared with other kinds of adsorbents, the

**Table 1** Adsorption capacities of different adsorbents for removal of methyl orange

Adsorbents	$Q_{\max}$ ( $\text{mg g}^{-1}$ )	References
Chitosan	34.8	[30]
Organo montmorillonite	47.8	[31]
$\gamma\text{-Fe}_2\text{O}_3/\text{MWCNTs}/\text{chitosan}$	66.1	[32]
Acid-modified carbon-coated monolith	147.1	[33]
Mesoporous magnetic Co-NPs/carbon nanocomposites	380.0	[34]
Chitosan/ $\text{Al}_2\text{O}_3$ /magnetite nanoparticles composite	416.0	[35]
QCS/MMT nanocomposite resin	478.5	This study
Graphene oxide-doped chitosan monoliths	567.1	[29]

adsorption capacity of QCMR is lower than that of graphene oxide-doped chitosan monoliths [29]. However, as a low-cost adsorbent, QCMR has higher methyl orange removal ability than chitosan [30], organo montmorillonite [31],  $\gamma\text{-Fe}_2\text{O}_3/\text{MWCNTs}/\text{chitosan}$  [32], acid-modified carbon-coated monolith [33], mesoporous magnetic Co-NPs/carbon nanocomposites [34], and chitosan/ $\text{Al}_2\text{O}_3$ /magnetite nanoparticles composite [35], reflecting its potential application in adsorption of organic contaminants.

## Conclusions

Novel quaternized chitosan/montmorillonite nanocomposite resin was successfully prepared. The resins showed a regularly spherical shape, dense structure and good dispersibility in water. Furthermore, since the quaternary ammonium salt encouraged the molecules to stretch, the swelling degree of several different resins decreased with the increase of pH values, and the swelling degree of the resin was lower with the addition of MMT, which is more suitable for the resin to pack column. Compared with quaternized chitosan resin, the adsorption capacity of QCMR enhances obviously, thanks to the addition of MMT. Within the range of experimental concentration, QCMR on the adsorption behavior of methyl orange can be well described by Langmuir and Freundlich adsorption isotherm models. Therefore, this study may provide a considerable and prospective material in the field of water treatment.

**Acknowledgments** This work was financially supported by the National Natural Science Foundation of China (No. 51403069, 41206035), the Program for New Century Excellent Talents in University (NCET-13-0216), the Scientific Research of Fund Project for Young Teachers, South China Normal University, open fund of State Key Laboratory of Pulp & Paper Engineering, South China University of Technology.



## References

- Wang Q, Du YM, Fan LH, Liu H, Wang XH (2003) Structures and properties of chitosan-starch-sodium benzoate blend films. *Wuhan Univ J Nat Sci* 6:725–730
- Yang Y, Wang SP, Wang YT, Wang XH, Wang Q, Chen MW (2014) Advances in self-assembled chitosan nanomaterials for drug delivery. *Biotechnol Adv* 32:1301–1316
- Ding FY, Deng HB, Du YM, Shi XW, Wang Q (2014) Emerging chitin and chitosan nanofibrous materials for biomedical applications. *Nanoscale* 6:9477–9493
- Yuan YH, Jia DM, Yuan YH (2013) Chitosan/sodium alginate, a complex flocculating agent for sewage water treatment. *Adv Mater Res* 641:101–104
- Jia F, Liu XP, Li LH, Mallapragada S, Narasimhan B, Wang Q (2013) Multifunctional nanoparticles for targeted delivery of immune activating and cancer therapeutic agents. *J Controlled Release* 172:1020–1034
- Peng HS, Liu XP, Wang R, Jia F, Dong L, Wang Q (2014) Emerging nanostructured materials for musculoskeletal tissue engineering. *J Mater Chem B* 2:6435–6461
- Hu XW, Tang YF, Wang Q, Li Y, Yang JH, Du YM, Kennedy JF (2011) Rheological behaviors of chitin in NaOH/urea aqueous solution. *Carbohydr Polym* 83:1128–1133
- Kawamura Y, Mitsuhashi M, Tanibe H, Yoshida H (1993) Adsorption of metal ions on polyaminated highly porous chitosan chelating resin. *Ind Eng Chem Res* 32:386–391
- Qin CQ, Du YM, Zhang ZQ, Liu Y, Xiao L, Shi XW (2003) Adsorption of chromium (VI) on a novel quaternized chitosan resin. *J Appl Polym Sci* 90:505–510
- Bhattacharyya KG, Gupta SS, Sarma GK (2015) Kinetics, equilibrium isotherms and thermodynamics of adsorption of Congo red onto natural and acid-treated kaolinite and montmorillonite. *Desalin Water Treat* 53:530–542
- Zhan YF, Zeng W, Jiang GX, Wang Q, Shi XW, Zhou ZH, Deng HB, Du YM (2015) Construction of lysozyme exfoliated rectorite-based electrospun nanofibrous membranes for bacterial inhibition. *J Appl Polym Sci* 132:41496
- Dias MV, Azevedo VM, Borges SV, Soares NDF, de Barros Fernandes RV, Marques JJ, Medeiros ÉAA (2014) Development of chitosan/montmorillonite nanocomposites with encapsulated  $\alpha$ -tocopherol. *Food Chem* 165:323–329
- Lewandowska K, Sionkowska A, Kaczmarek B, Furtos G (2014) Mechanical and morphological studies of chitosan/clay composites. *Mol Cryst Liq Cryst* 590:193–198
- Liu B, Wang XY, Yang B, Wang XH, Sun RC (2011) Microwave irradiation-assisted synthesis and flocculation behavior of quaternized chitosan/organo-montmorillonite nanocomposite. *Curr Nanosci* 7:1034–1041
- Liu B, Shen SQ, Luo JW, Wang XY, Sun RC (2013) One-pot green synthesis and antimicrobial activity of exfoliated Ag NP-loaded quaternized chitosan/clay nanocomposites. *Rsc Adv* 3:9714–9722
- Wang XY, Du YM, Luo JW (2008) Biopolymer/montmorillonite nanocomposite: preparation, drug-controlled release property and cytotoxicity. *Nanotechnol* 19:065707
- Annadurai G, Juang RS, Lee DJ (2002) Use of cellulose-based wastes for adsorption of dyes from aqueous solutions. *J Hazard Mater* 92:263–274
- Celis R, Adelino MA, Hermosin MC, Cornejo J (2012) Montmorillonite-chitosan bionanocomposites as adsorbents of the herbicide clopyralid in aqueous solution and soil/water suspensions. *J Hazard Mater* 209:67–76
- Van der Marel HW, Beutelspacher H (1976) Atlas of infrared spectroscopy of clay minerals and their admixtures. Elsevier Publishing Company
- Li XY, Liu B, Ye WJ, Wang XY, Sun RC (2015) Effect of rectorite on the synthesis of Ag NP and its catalytic activity. *Mater Chem Phys* 151:301–307
- Xu LN, Lv FZ, Zhang YH, Luan XL, Zhang Q, An Q (2014) Interfacial modification of magnetic montmorillonite (MMT) using covalently assembled LbL multilayers. *J Phys Chem C* 118:20357–20362
- Han GC, Han Y, Wang XY, Liu SJ, Sun RC (2014) Synthesis of organic rectorite with novel Gemini surfactants for copper removal. *Appl Surf Sci* 317:35–42
- Qin CQ, Xiao L, Du YM, Shi XW, Chen JW (2002) A new cross-linked quaternized-chitosan resin as the support of borohydride reducing agent. *React Funct Polym* 50:165–171
- Kim JH, Lee YM (1993) Synthesis and properties of diethylaminoethyl chitosan. *Polymer* 34:1952–1957
- Shtarker-Sasi A, Castro-Sowinski S, Matan O, Kagan T, Nir S, Okon Y, Nasser AM (2013) Removal of bacteria and *Cryptosporidium* from water by micelle-montmorillonite complexes. *Desalin Water Treat* 51:7672–7680
- Ren XH, Zhang ZL, Luo HJ, Hu BJ, Dang Z, Yang C, Li LY (2014) Adsorption of arsenic on modified montmorillonite. *Appl Clay Sci* 97:17–23
- Hiwarkar AD, Srivastava VC, Mall ID (2014) Simultaneous adsorption of nitrogenous heterocyclic compounds by granular activated carbon: parameter optimization and multicomponent isotherm modeling. *Rsc Adv* 4:39732–39742
- Luo JW, Wang XY, Xia B, Wu J (2010) Preparation and characterization of quaternized chitosan under microwave irradiation. *J Macromol Sci Part A Pure Appl Chem* 47:952–956
- Wang Y, Liu X, Wang H, Xia G, Huang W, Song R (2014) Microporous spongy chitosan monoliths doped with graphene oxide as highly effective adsorbent for methyl orange and copper nitrate ( $\text{Cu}(\text{NO}_3)_2$ ) ions. *J Colloid Interface Sci* 416:243–251
- Saha TK, Bhoumik NC, Karmaker S, Ahmed MG, Ichikawa H, Fukumori Y (2010) Adsorption of methyl orange onto chitosan from aqueous solution. *J Water Resour Prot* 2:898–906
- Liu B, Wang XY, Yang B, Sun RC (2011) Rapid modification of montmorillonite with novel cationic Gemini surfactants and its adsorption for methyl orange. *Mater Chem Phys* 130:1220–1226
- Zhu HY, Jiang R, Xiao L, Zeng GM (2010) Preparation, characterization, adsorption kinetics and thermodynamics of novel magnetic chitosan enwrapping nanosized  $\gamma\text{-Fe}_2\text{O}_3$  and multi-walled carbon nanotubes with enhanced adsorption properties for methyl orange. *Bioresour Technol* 101:5063–5069
- Cheah W, Hosseini S, Khan MA, Chuah TG, Choong TS (2013) Acid modified carbon coated monolith for methyl orange adsorption. *Chem Eng J* 215:747–754
- Zhang P, An Q, Guo J, Wang CC (2013) Synthesis of mesoporous magnetic Co-NPs/carbon nanocomposites and their adsorption property for methyl orange from aqueous solution. *J Colloid Interface Sci* 389:10–15
- Tanhaei B, Ayati A, Lahtinen M, Sillanpää M (2015) Preparation and characterization of a novel chitosan/ $\text{Al}_2\text{O}_3$ /magnetite nanoparticles composite adsorbent for kinetic, thermodynamic and isotherm studies of methyl orange adsorption. *Chem Eng J* 259:1–10